NASA TECHNICAL NOTE

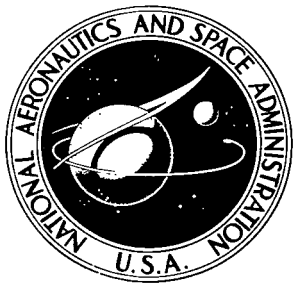

EVALUATION OF AN ABNORMAL-GLOW DISCHARGE FOR USE AS A LABORATORY PLASMA SOURCE

by Albert S. Roberts, Jr., and William L. Grantham

Langley Research Center
Hampton, Va. 23365

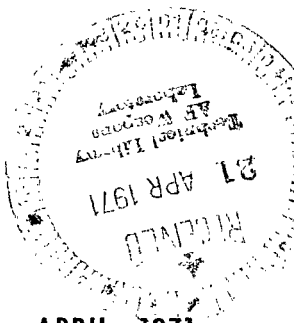

NATIONAL AERONAUTICS AND SPACE ADMINISTRATION • WASHINGTON, D. C. • APRIL 1971

1. Report No.	2. Government Accession No.	3. Recipient's Catalog No.
NASA TN D-6136		

4. Title and Subtitle	5. Report Date
EVALUATION OF AN ABNORMAL-GLOW DISCHARGE FOR USE AS A LABORATORY PLASMA SOURCE	April 1971
	6. Performing Organization Code

7. Author(s)	8. Performing Organization Report No.
Albert S. Roberts, Jr. (Old Dominion University) and William L. Grantham	L-6912
	10. Work Unit No.
9. Performing Organization Name and Address	125-21-21-01
NASA Langley Research Center Hampton, Va. 23365	11. Contract or Grant No.
	13. Type of Report and Period Covered
12. Sponsoring Agency Name and Address	Technical Note
National Aeronautics and Space Administration Washington, D.C. 20546	14. Sponsoring Agency Code

15. Supplementary Notes

16. Abstract

Abnormal-glow-discharge plasmas from both needle- and inverted-brush cathode configurations were studied for potential use as laboratory test beds to develop and calibrate plasma diagnostic sensors. Electron densities of 10^{12} electrons/cm^3 were produced with short-term variations of less than ±6 percent and long-term (several months) repeatability better than ±15 percent.

Measured plasma profiles are in good agreement with linear diffusion theory for uniformly spaced brush elements; however, an attempt to shape the steady-state profile by tailoring the cathode distribution did not produce the theoretically predicted result. During tube warmup, some profile shaping was observed.

17. Key Words (Suggested by Author(s))	18. Distribution Statement
Abnormal-glow discharge Negative glow Laboratory plasma source Langmuir probe Microwave interferometer	Unclassified – Unlimited

19. Security Classif. (of this report)	20. Security Classif. (of this page)	21. No. of Pages	22. Price*
Unclassified	Unclassified	29	$3.00

*For sale by the National Technical Information Service, Springfield, Virginia 22151

EVALUATION OF AN ABNORMAL-GLOW DISCHARGE FOR USE AS A LABORATORY PLASMA SOURCE

By Albert S. Roberts, Jr.*, and William L. Grantham
Langley Research Center

SUMMARY

Abnormal-glow-discharge plasmas from both needle- and inverted-brush cathode configurations were studied for potential use as laboratory test beds to develop and calibrate plasma diagnostic sensors. Electron densities of 10^{12} electrons/cm^3 were produced with short-term variations of less than ±6 percent and long-term (several months) repeatability better than ±15 percent.

Measured plasma profiles are in good agreement with linear diffusion theory for uniformly spaced brush elements; however, an attempt to shape the steady-state profile by tailoring the cathode distribution did not produce the theoretically predicted result. During tube warmup, some profile shaping was observed.

INTRODUCTION

The development of new and improved plasma measurement techniques requires better laboratory plasmas. A variety of plasma sources have been used in the past for evaluating plasma diagnostic techniques. In reference 1, a shock tube was used to evaluate electrostatic probes intended for reentry plasma measurements. In references 2 and 3, microwave diagnostic techniques were evaluated in a radiofrequency-generated plasma source and gaseous discharge tube.

A plasma source which has several improved properties (stability and repeatability) that make it especially suitable as a test bed for evaluating new diagnostic techniques has been described by Persson (ref. 4). These properties were possible through his studies of an abnormal-glow discharge from a multineedle-brush cathode. His particular cathode configuration extended the length of the negative-glow plasma, which characteristically has a more stable and repeatable electron density than other available sources.

*Associate Professor of Engineering, Old Dominion University, Norfolk, Va. (Consultant at NASA Langley Research Center).

Experiments by Musal (ref. 5) demonstrated the use of an inverted-brush cathode in a cold-cathode discharge. With both the needle-brush and inverted-brush cathodes, a stable plasma environment was produced with electron densities exceeding 10^{12} electrons/cm^3. References 6 and 7 also report experimental results obtained with a negative-glow plasma.

Cylindrical cathodes used in this experiment are similar to those used by Persson and Musal. A modified rectangular cathode made of alternately long and short laminations was also studied. The composition, density, and temperature structure of electron-beam-generated plasmas have not yet been adequately analyzed; however, several important papers treating the basic physics are in references 8 to 14.

Four specific objectives were desired in the work presented herein: (1) to produce a static plasma that is free of large variations in electron density n_e (with $n_e > 10^{11}$ cm^{-3}); (2) to obtain reproducible, reliable values of electron density and electron temperature T_e; (3) to obtain the spatial distribution of the electron density for correlation with theoretical profiles; and (4) to control transverse electron-density profiles to give a nearly uniform distribution in the plane perpendicular to the tube axis. All these objectives are aimed at providing a known and controllable plasma environment for studying antenna-plasma interactions (ref. 15).

Measurements of the plasma electron density were made with microwave interferometers and Langmuir probes. The interferometer is considered more accurate because of the ease of interpreting the phase data and because dielectric calibration techniques could be used to check its accuracy. The Langmuir probe data, which are more difficult to interpret in terms of absolute electron density, were used primarily to measure electron-density profile shape and electron temperature.

SYMBOLS

a	length of rectangular cathode, cm
b	height of rectangular cathode, cm
c	speed of light, m/sec
D_a	ambipolar diffusion coefficient, cm^2/sec
e	electron charge, coulombs (C)
H	unit step function

i	normalized saturation ion current (normalized to value at tube center)
k	integer
l	integer
m	mass, kg
n_e	electron number density, cm^{-3}
p	pressure, torr $\left(1 \text{ torr} = 133.3 \text{ N/m}^2\right)$
r	radial distance from tube center, cm
R	radius of circular tube, cm
S	electron source term of cathode surface, $cm^{-3}\text{-}sec^{-1}$
S_o	electron source term of unmodified cathode surface, $cm^{-3}\text{-}sec^{-1}$
T	temperature, ^oC or ^oK
V	voltage, volts (V)
x,y	rectangular coordinates used in description of cathode, cm
α	recombination coefficient, cm^3/sec
ϵ_o	permittivity of free space, C/V-m
θ	fraction of electron source term excluded due to insulator
λ_D	Debye wavelength, cm
ω	electromagnetic frequency, rad/sec

Subscripts:

at	atom

e	electron
i	ion
j	index for variable
1	identifies specific value of variable

APPARATUS AND MEASUREMENT TECHNIQUES

Cylindrical Plasma Tube

General features of the discharge tube and associated apparatus are shown in figures 1 and 2. End plates with service penetrations close off the large (45.7-cm diameter) tube which houses the smaller discharge tube. Equal pressures inside and outside the small discharge tube permit the use of thin tube walls needed for studies of antenna-plasma interaction.

The discharge tube used in the negative-glow plasma experiments was operated as a continuously pumping vacuum system. A leak valve and a 7.1×10^{-3} m^3/sec mechanical vacuum pump allowed constant-pressure operation. Before the cold-cathode, direct-current discharge was initiated, the system was pumped to less than 10^{-3} torr. Several helium purges up to 10 torr were performed to limit impurity content; however, neither cryogenic nor chemical trapping was used on the vacuum pump or gas inlet lines. Pressure was determined within ±6 percent over the operating range of the discharge tube (0.92 to 1.4 torr). Pressure drift was kept below 6 percent during the test period since greater changes might cause a measurable change in plasma properties.

A well-regulated, low-ripple (0.01 percent V rms) dc power supply was used to drive the discharge. Power levels of 100 to 200 watts were sufficient to operate the abnormal-glow discharge at 2 kV and 1 to 2 torr. Stability of the power supply was important to prevent time-varying plasma electron density.

A primary design problem involved careful suppression of electrical breakdown at the cathode support plate. A teflon gasket (fig. 2(b)) was used to insulate the cathode from the stainless-steel end plate (ground) and provide a resilient seat for the pyrex tube, which fitted closely about the cathode. The pyrex tube (48.5 cm long) was spring-loaded from the anode end to allow for thermal expansion. Helium, fed through a pyrex tube near the base of the cathode, was slowly pumped out through vents in the anode.

A tungsten-needle-brush cathode and inverted-brush cathode were constructed for use in the abnormal-glow discharge (fig. 3). Fabrication of the needle brush was a more

difficult task, since several thousand tungsten needles (0.127 cm in diameter and 3.94 cm long) had to be brazed into a stainless-steel base plate. For a given tube voltage, the tube current for the inverted-brush cathode was higher than that for the needle-brush cathode and the inverted-brush cathode took longer to reach equilibrium. Short thermal-equilibrium time was needed; therefore, the needle-brush cathode was used in subsequent experiments.

Rectangular Plasma Tube

The objectives cited in the Introduction will now be applied with some additional considerations to make the rectangular tube more suitable for antenna-plasma studies. These include the need for a greater volume of plasma with a more uniform density and control of the transverse plasma profile.

The rectangular plasma tube was assembled with precision-ground quartz plates arranged to form a parallelepiped about a rectangular cathode; dimensions were $19.05 \times 6.35 \times 45.7$ cm measured along inside surfaces. Figure 4 depicts the rectangular cathode composed of 0.16-cm-wide niobium laminae of two different heights. This modified brush design provided a large cathode surface area; furthermore, the cathode composition could be varied in the thin dimension by replacing niobium laminae with a nonconductor (Lavite, for example). Such an exchange has been made in the brush cathode shown in figure 5 in an effort to control the shape of the electron-density profile. Niobium was chosen as a cathode material because of its low sputter coefficient under ion bombardment.

Plasma Diagnostics

Since the plasma under evaluation is intended primarily for studies of microwave-antenna—plasma interaction, the plasma property of interest is electron density and its spatial distribution. Both microwave interferometers and Langmuir probes were used to measure electron density. The interferometer data, in this particular case, are more accurate than the wire probe data because of a simple conversion of phase data to electron density and because of calibrations used to verify the accuracy of the interferometer.

Microwave interferometer.- A 20-GHz interferometer was used to measure plasma phase shift. Figures 2 and 6 show a photograph and schematic of the microwave-interferometer installation. The microwave antennas were installed inside the main vacuum chamber; copper tubes with an inside diameter of 1.27 cm served as waveguides, and penetrations for these were made in the stainless-steel end plate. The antennas could be placed at any location along the axis of the tube as needed. Three different locations were used in these experiments.

The interferometer accuracy was checked by using dielectric slabs of known permittivity between the antennas. This not only checked the measurement accuracy of the system but qualified the measurements for interpretation with the use of plane-wave theory (refs. 16 and 17). The calibrations were made with the discharge tube in place. A 48-GHz interferometer was used during some experiments and confirmed the n_e values obtained with the 20-GHz system within 12 percent.

The measured phase $\Delta\varphi$ was used to determine electron density from the following equation (eq. 4.2.3, in ref. 17): $\Delta\varphi = \frac{e^2 \times 10^6}{2\epsilon_0 mc\omega} \int n(x)\, dx$. In all experiments the plasma density was less than 2×10^{12} cm^{-3}, which is well below critical density for the frequencies 20 and 48 GHz (approximately 5×10^{12} cm^{-3} and 3×10^{13} cm^{-3}, respectively). Since plasma densities were well below the critical value, the phase parameter was easily integrated (ref. 17) to establish a density correlation; a parabolic spatial distribution of n_e was assumed. This density distribution is confirmed to be parabolic by Langmuir probe data presented later in this report.

Langmuir probe.- Langmuir probes were used to obtain high spatial resolution necessary for measurements of electron-density profiles. Analysis of the electric-probe data is not as straightforward as that of interferometer data and is, therefore, discussed in more detail.

A microscopic approach must be taken in order to analyze the electric current to a wire probe immersed in a plasma in terms of electron density and electron temperature. A self-consistent analysis for a current-collecting probe has been developed by Laframboise (ref. 18) with the assumption of no interparticle collisions in the sheath region between the plasma and a cylindrical probe surface. Sonin (ref. 19) adapted this technique for the experimentalist, and a further adaptation of the Laframboise results was incorporated in the computer program for the present paper to compute n_e and T_e from the Langmuir probe signatures.

To interpret Langmuir probe data, the experimentalist should know about collisional processes in the vicinity of the probe, electric potential distribution in the sheath, and the characteristic plasma dimensions, such as mean free paths relative to probe size. A report by Kanal et al. (ref. 20) describes the sheath structure quantitatively and presents physically realistic potential models which are compared with the results of Laframboise. Table I lists values of mean-free-paths, Debye length λ_D, and other characteristic lengths for the negative glow plasma in helium at 1.2 torr. The fact that the Debye length, which is a measure of sheath thickness, is larger than the probe radius allows accelerated particle orbits that may not intersect the probe surface. Also, the ion-atom and ion-ion mean free paths are not large compared with sheath thickness; thus, multiple collisions in the sheath are possible. Since density measurements from the Langmuir probe did have

increasingly better agreement with interferometer measurements as probe radii were reduced (from 254 μm to 127 μm, 76.2 μm, 25.4 μm, and 7.62 μm), it can be assumed that there were orbits and collisions in the probe sheaths. Length-to-diameter ratios for the tungsten wire probes were made about 100 for all probes to minimize end effects.

The small probes were the most difficult to fabricate. Serviceable probes were made either by drawing pyrex down onto the wire and trimming, or for the finer wires, by using an oven-glazed silicone cement to seal the end of the pyrex tube around the wire. This wire probe was inserted from the anode end of the tube and its end located directly between the two microwave antennas.

Two degrees of freedom were available for transverse Langmuir probe motion without disassembling the tube by using a mechanical linkage from the probe mount inside the vacuum chamber to exterior controls. A nine-point transverse profile could be taken in about 20 minutes. The glass-sheathed probes could also be retracted for measurements at different axial positions. Before probe signatures were taken, the probe was cleaned by drawing sufficient electron current to bake it out at a dull white glow. This procedure gave better reproducibility of the current-voltage signatures.

After the probe was positioned, data were obtained by sweeping the voltage on the probe plus and minus several volts around the floating potential. Voltage and current to the probe were recorded by use of the circuit shown in figure 7. Probe signatures, probe dimensions, gas properties, and measured ion temperature were punched onto cards for subsequent computation of n_e and T_e with a digital computer program.

EXPERIMENTAL RESULTS AND DISCUSSION

Circular-Brush-Cathode Plasma

Operating data for the tube with the circular brush cathode are shown in figure 8. The positive slope of the voltage-current curve is the expected characteristic of an abnormal-glow discharge (ref. 21). In this abnormal mode, the negative-glow region of the discharge was extended down the tube, had a characteristic pink deexcitation light, and had a floating potential of a few volts (positive-column regions normally have 50 volts or more).

The region of negative-glow plasma is produced by a low-density beam of electrons emitted from the cathode when the needle surfaces are bombarded by positive ions. The electron beam has, to a first approximation, a kinetic energy equivalent to the cathode potential, and most of the tube potential drop occurs near the cathode. Adjustment of tube voltage affected the reaching distance of the primary electron beam, as evidenced by the change observed in the length of the pink negative-glow region.

Electron density measurements.- Interferometer data shown in figure 9 indicate the measured levels of plasma electron density for different tube conditions. The electron-density levels are especially sensitive to pressure around 1.1 torr. Good repeatability (±15 percent) of electron concentration was observed over a period of several months, and the short-term variations were less than ±6 percent. Warmup of the tube required about 30 minutes and appeared to be related to the temperature of the cathode. All data were taken after this warmup time so that the plasma properties would be stable. A comparison of interferometer and Langmuir probe (7.62-μm diameter) data is given in figure 10 for different tube conditions. These data show that although the curves are similar in general shape, they are quite different in magnitude. The Langmuir probe data are generally lower than microwave values. (See ref. 6.)

It should be kept in mind that the primary data needed from Langmuir probes are the shapes of the n_e profiles and that absolute values of n_e are obtained from the interferometer.

Electron-density profiles.- Theoretical calculations of radial electron-density profiles have been made by Persson (ref. 4) for the negative-glow plasma. A simplified ambipolar diffusion treatment was used, wherein the governing equation for electron density with axial gradients neglected is

$$D_a \frac{1}{r} \frac{\partial\left(r\frac{\partial n_e}{\partial r}\right)}{\partial r} + S = \alpha n_e^2 \tag{1}$$

with

$$\frac{\partial n_e}{\partial r} = 0 \quad \text{at} \quad r = 0 \text{ (center line)}$$

and

$$n_e = 0 \quad \text{at} \quad r = R \text{ (wall)}$$

In this equation, S is a uniform source term due to the primary electron beam, D_a is the ambipolar diffusion coefficient, and α is a volume recombination coefficient. The validity of some inherent assumptions in this model have been discussed in another paper by Persson (ref. 13). The solution of equation (1) results in a radial profile that is parabolic, since the n_e distribution is diffusion limited (i.e., $\alpha n_e^2 = 0$, ref. 4). Subsequent experiments show that the profile was, in fact, parabolic.

Profile data taken with the Langmuir probe at a fixed axial station are shown in figure 11; tube pressure and voltage are specified. These data show the reproducibility of density profiles (radial), since the data shown (runs 28, 32, and 45) were taken over a 14-day period. Note the discrepancy between the density measured by the microwave interferometer and the Langmuir probe on the tube center line. Also shown in figure 11

is the theoretical profile computed with the simplified ambipolar diffusion model of Persson (ref. 4). The good comparison of theory and experiment gives added confidence in the theoretical model. Profiles taken with several different probe diameters always gave the same profile shape even though the magnitudes of n_e were very different.

Density profile shapes were reproducible, but the local values of electron temperature T_e varied by as much as 33 percent at any given operating condition. Steady-state gas temperatures were 90^o to 100^o C as measured by a thermocouple at the tube wall (fig. 12). Gas and ion temperatures are assumed to be the same. There is little coupling between random energy modes via electron-ion collisions; hence, T_e is strongly influenced by other volume effects. Heating of the plasma electrons is most probably caused by destruction of metastable atoms in collisional-radiative recombination events with the plasma electron acting as a third body (ref. 11). Measured electron temperatures ranged from 3000^o to 5000^o K, which are higher than those reported by Powers (ref. 22) for a negative glow in high-purity helium.

For any given tube operating conditions, the repeatability of T_e was about 33 percent (derived from the Langmuir probe). Even so, experiments showed that a variation of 33 percent in local electron temperature, used in the reduction of the Langmuir probe data, changed the corresponding n_e by only 4 percent. In Persson's negative-glow plasma, electron temperatures were lower by a factor of 2 or 3 than those reported herein.

Rectangular-Cathode Plasma

The rectangular cathode resulted in negative-glow plasma that was very stable with the laminated cathode configuration, and the cathode was less susceptible to sparking. The operating voltage ranged closely around 2 kV, and tube current increased in proportion to the area increase over that of the circular brush cathode. Parametric data taken by varying pressure and voltage showed similar trends and magnitudes when compared with the circular-tube data.

The neutral gas temperature in the discharge was monitored as a function of time from a cold startup. The tube current and electron density changed with the gas temperature until a steady-state temperature was reached. Repeatable plasma data were obtained only after this equilibrium was obtained. The coupling mechanism between long-time tube warmup and short-relaxation-time plasma properties is not presently well understood. Time needed to obtain equilibrium was substantially longer for the rectangular configuration as shown in figure 12.

Profile data taken at three axial stations are shown in figure 13. These Langmuir probe data have been adjusted so that the center value agrees with the microwave-interferometer value. Off-center values were also adjusted by the same factor. Further

study is required to determine whether the skewed profile at the axial location 26.04 cm from the cathode is a real effect or is due to data inaccuracy.

In figure 14, density profile data are shown to correlate well with linear theory (diffusion limited) for the axial distance of 20.95 cm. In this case the theoretical profile was obtained from the solution of

$$D_a\left(\frac{\partial^2 n_e}{\partial x^2} + \frac{\partial n_e}{\partial y^2}\right) + S = 0 \tag{2}$$

Agreement between theory and experiment is better for the rectangular-tube data than for the circular-tube data (fig. 11).

Control of the transverse spatial plasma distribution was needed to make the plasma more versatile. The approach taken was based on physical interpretation of the plasma source mechanism, operative through a primary electron beam emanating from the cathode. Since volume ionization is produced by this beam, a variation in cathode surface emission could be expected to redistribute the plasma.

To determine whether there would be any redistribution, computations of the transverse electron-density profile (fig. 15) were made based on the solution of equation (2) with a variable source term. The solution to equation (2), derived in the appendix, is

$$n_e(x,y) = \frac{\alpha^2 S_o}{D_a} \sum_{k=1}^{\infty} \sum_{l=1}^{\infty} \frac{\frac{16}{\pi^4}\left(1 - \theta \cos \frac{l\pi b_1}{b}\right) \sin \frac{k\pi x}{a} \sin \frac{l\pi y}{b}}{kl\left[k^2 + \left(\frac{ab}{b}\right)^2\right]} \tag{3}$$

where k and l can assume odd values only. The width and height of the cathode are a and b, and S_o is the source term for the unmodified portion of the cathode. The parameter θ, which is a fraction of the uniform source, is described in the appendix. For $\theta = 1.0$, no electron emission is permitted from the dielectric portion of the cathode; hence, the hollow beam source cathode (fig. 5) should cause a flattened electron-density profile if the analysis is correct. The effect of electric fields normal to the electron beam was not considered.

Experiments were performed with the segmented cathode, but the steady-state, thermal-equilibrium results displayed no flattened profile. The results indicate only some asymmetry and a decrease in electron density. However, during tube warmup a less peaked distribution in the y-direction was observed. This observation is indicated in figure 16 where ion current is shown as a function of vertical distance from the tube center. For an isothermal plasma, the ion current is proportional to the electron density. Cryogenically cooled helium was leaked through the gas inlet to see whether the profile shaping could be preserved for a longer time. Using the cooled helium extended the equilibration time to about 3 hours.

CONCLUDING REMARKS

A stable, negative-glow plasma with reproducible properties has been achieved. This plasma has repeatable electron densities within ±15 percent over a period of several months and short-term stability of ±6 percent. Electron-density profiles determined from Langmuir probe measurements have the same shape as predicted with linear diffusion theory. Attempts to control the electron-density profile by shaping the rectangular cathode were only partially successful.

Correlation of electron concentrations determined by the microwave interferometer and the Langmuir probe is best for the smallest probe used (7.6 μm in diameter). Errors in excess of 50 percent were experienced with larger probes.

During this study some significant problem areas have been uncovered and deserve further attention. The two most interesting anomalies encountered during the research were (1) disagreement of electron-density values measured by the Langmuir probe and the microwave interferometer (these values were resolved within a factor of 2) and (2) the effect of tube warmup on magnitude and distribution of plasma density. The first problem requires further consideration regarding applicability of collisionless electric-probe theory; the second problem indicates the need for theoretical and experimental transient analysis. From an applications standpoint these two problems can be tolerated. For example, although there are differences in magnitudes of election density (depending on probe radius), the electron-density profile shapes are independent of probe radius and tube pressure.

Langley Research Center,
National Aeronautics and Space Administration,
Hampton, Va., January 19, 1971.

APPENDIX

DIFFUSION-EQUATION SOLUTION

Solution of the diffusion equation (2) was determined for the rectangular discharge tube to obtain the two-dimensional electron-density distribution given as equation (3). Generation of plasma was assumed to vary directly with the area of the cathode face from which the primary electron beam was emitted. A technique of finite Fourier integral transformations was used to obtain the series solution for $n_e(x,y)$.

Consider the model outlines in sketch 1.

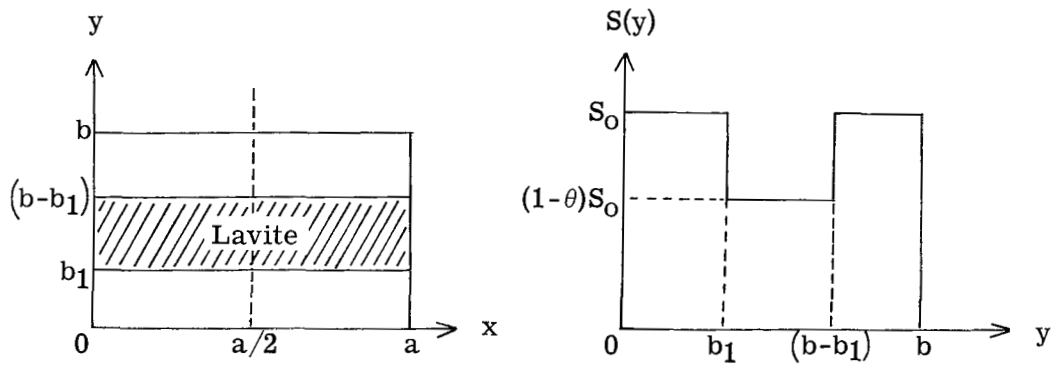

Cathode face

Source distribution along a/2

Sketch 1

The coordinate $y = b_1$ locates the edge of the Lavite insulator, where $0 < b_1 \leqq b/2$. The parameter θ is the fraction of the uniform source S_o which is excluded because of the insulator, where $0 \leqq \theta \leqq 1$. In terms of unit step functions the distributed source term for equation (2) can be written as

$$S(y) = S_o\Big\{H(y) - \theta H(y - b_1) + \theta H\big[y - (b - b_1)\big] - H(y - b)\Big\} \tag{A1}$$

where

$$H(y - y_j) = 0 \qquad (y \leqq y_j)$$

and

$$H(y - y_j) = 1 \qquad (y > y_j)$$

The four boundary conditions for electron number density required for solution of equation (2) are

$$\left.\begin{aligned} n_e(0,y) &= n_e(a,y) = 0 \\ n_e(x,0) &= n_e(x,b) = 0 \end{aligned}\right\} \tag{A2}$$

Formal transformation of equations (2) is made by defining certain integral functions. This method of solving a partial differential equation is discussed in reference 23. Define successive finite sine transforms $\bar{n}_e$ and $\bar{\bar{n}}_e$ of the number density as follows:

$$\bar{n}_e(k,y) = \int_0^a n_e(x,y) \sin \frac{k\pi x}{a}\, dx \tag{A3}$$

$$\bar{\bar{n}}_e(k,l) = \int_0^b \bar{n}_e(k,y) \sin \frac{l\pi y}{b}\, dy \tag{A4}$$

Multiplying equations (2) successively by $\sin \frac{k\pi x}{a}\, dx$ and $\sin \frac{l\pi y}{b}\, dy$ and successively integrating by parts by use of equations (A3) and (A4) gives the following equation in k- and l-space:

$$\bar{\bar{n}}_e(k,l) = \int_0^b \int_0^a \frac{S(y) \sin \frac{k\pi x}{a} \sin \frac{l\pi y}{b}\, dx\, dy}{D_a \pi^2 \left(\frac{k^2}{a^2} + \frac{l^2}{b^2}\right)} \tag{A5}$$

Substituting for $S(y)$ from equation (A1) and integrating equation (A5) leads to

$$\bar{\bar{n}} = \frac{S_o ab\left[1 + (-1)^{l+1}\right]\left[1 + (-1)^{k+1}\right]\left(1 - \theta \cos \frac{l\pi b_1}{b}\right)}{\pi^4 \left(\frac{k^2}{a^2} + \frac{l^2}{b^2}\right) D_a k l} \tag{A6}$$

When inversion theorems for Fourier transformations are employed, a solution is obtained in terms of a double summation with the transform variables k and l as indices:

$$n_e(x,y) = \frac{4}{ab} \sum_{k=1}^{\infty} \sum_{l=1}^{\infty} \bar{\bar{n}}_e(k,l) \sin \frac{k\pi x}{a} \sin \frac{l\pi y}{b} \tag{A7}$$

where k and l run through all integers. Substituting equation (A6) into (A7) leads to

$$n_e(x,y) = \frac{a^2 S_o}{D_a} \sum_{k=1}^{\infty} \sum_{l=1}^{\infty} \frac{\frac{16}{\pi^4}\left(1 - \theta \cos \frac{l\pi b_1}{b}\right) \sin \frac{k\pi x}{a} \sin \frac{l\pi y}{b}}{kl\left[k^2 + \left(\frac{ab}{b}\right)^2\right]}$$

where k and l can now assume odd values only. This series solution was summed on a digital computer and boundary conditions were checked. For the calculations of the normalized theoretical n_e profile in figure 15, the following values from sketch 1 were used: $x = \frac{a}{2}$, $\frac{b_1}{b} = \frac{1}{4}$, and $\frac{b}{a} = \frac{1}{4}$.

REFERENCES

1. Scharfman, W. E.; and Bredfeldt, H. R.: Use of the Langmuir Probe To Determine The Electron Density and Temperature Surrounding Re-Entry Vehicles. SRI Project 5771 (Contract NAS 1-4872), Stanford Res. Inst., Dec. 1966. (Available as NASA CR-66275.)

2. Croswell, William F.; Taylor, William C.; Swift, C. T.; and Cockrell, Capers R.: The Input Admittance of a Rectangular Waveguide-Fed Aperture Under an Inhomogeneous Plasma: Theory and Experiment. IEEE Trans. Antennas Propagation, vol. AP-16, no. 4, July 1968, pp. 475-487.

3. Galejs, Janis; and Mentzoni, Michael H.: Waveguide Admittance for Radiation Into Plasma Layers – Theory and Experiment. IEEE Trans. Antennas Propagation, vol. AP-15, no. 3, May 1967, pp. 465-470.

4. Persson, Karl-Birger: Brush Cathode Plasma – A Well-Behaved Plasma. J. Appl. Phys., vol. 36, no. 10, Oct. 1965, pp. 3086-3094.

5. Musal, Henry M., Jr.: An Inverse Brush Cathode for the Negative-Glow Plasma Source. J. Appl. Phys., vol. 37, no. 4, Mar. 15, 1966, pp. 1935-1937.

6. Anderson, J. M.: Ultimate and Secondary Electron Energies in the Negative Glow of a Cold-Cathode Discharge in Helium. J. Appl. Phys., vol. 31, no. 3, Mar. 1960, pp. 511-515.

7. Anderson, J. M.; and Harris, L. A.: Negative Glow Plasma as a Cathode for Electron Tubes. J. Appl. Phys., vol. 31, no. 8, Aug. 1960, pp. 1463-1468.

8. Halsted, A. S.: Equilibrium Conditions and Beam Focusing Effects in a Beam-Generated Plasma. Rep. SUIPR No. 10 (Contract DA28-043-AMC-00482 (E)), Stanford Univ., June 1965.

9. Hurt, W. B.: Calculated Ion Distributions in a Helium Negative Glow. J. Chem. Phys., vol. 45, no. 9, Nov. 1, 1966, pp. 3439-3441.

10. Hurt, W. B.; and Robertson, W. W.: Atomic and Molecular Emission in the Negative Glow of a Helium Discharge. J. Chem. Phys., vol. 42, no. 2, Jan. 15, 1965, pp. 556-560.

11. Mosburg, Earl R., Jr.: Recombination of He^{+} and He^{++} in the Afterglow of a Helium Discharge. Phys. Rev., ser. 2, vol. 152, no. 1, Dec. 2, 1966, pp. 166-176.

12. Mosburg, Earl R., Jr.: Nonlinear Diffusion With Recombination in an Electron Beam Excited Plasma. Phys. Fluids, vol. 9, no. 4, Apr. 1966, pp. 824-826.

13. Persson, Karl-Birger: Inertia-Controlled Ambipolar Diffusion. Phys. Fluids, vol. 5, no. 12, Dec. 1962, pp. 1625-1632.

14. Self, S. A.; and Ewald, H. N.: Static Theory of a Discharge Column at Intermediate Pressures. Phys. Fluids, vol. 9, no. 12, Dec. 1966, pp. 2486-2492.

15. Sims, Theo E.: Communication Through Reentry Plasma. Conference Record – 1966 IEEE Winter Convention on Aerospace & Electronic Systems, Vol. I, IEEE, c.1966, pp. IB-21 – IB-28.

16. Wharton, Charles B.: Microwave Techniques. Plasma Diagnostic Techniques, Richard H. Huddlestone and Stanley L. Leonard, eds., Academic Press, Inc., 1965, pp. 477-516.

17. Heald, M. A.; and Wharton, C. B.: Plasma Diagnostics With Microwaves. John Wiley & Sons, Inc., c.1965.

18. Laframboise, James G.: Theory of Spherical and Cylindrical Langmuir Probes in a Collisionless, Maxwellian Plasma at Rest. Rep. No. 100, Inst. Aerosp. Studies, Univ. of Toronto, June 1966. (Available from DDC as AD 634 596.)

19. Sonin, A. A.: The Behavior of Free Molecular Cylindrical Langmuir Probes in Supersonic Flows, and Their Application to the Study of the Blunt Body Stagnation Layer. UTIAS Rep. No. 109, Univ. of Toronto, Aug. 1965.

20. Kanal, M.; Dow, W. G.; and Fontheim, E. G.: Volt-Ampere Characteristics of Cylindrical and Spherical Langmuir Probes for Various Potential Models. 06106-8-T (Grant No. NsG-525), College Eng., Univ. of Michigan, 1967.

21. Cobine, James Dillion: Gaseous Conductors. Dover Publ., Inc., c.1958, pp. 205-289.

22. Powers, Robert S., Jr.: Comparison of Langmuir Probe and Spectrometric Electron Temperature Measurements. J. Appl. Phys., vol. 37, no. 10, Sept. 1966, pp. 3821-3826.

23. Sneddon, Ian N.: Fourier Transforms. First ed., McGraw-Hill Book Co., Inc., 1951.

TABLE I.- TYPICAL CHARACTERISTIC LENGTHS OF BRUSH CATHODE PLASMA

[n_e (at tube center) = 10^{12} cm^{-3}; T_e = 4000° K;
$T_{at} \approx T_i$ = 400° K; p = 1.2 torr of He]

Probe radius, cm	0.00038
Ratio of probe length to diameter	100-200
Tube diameter, cm	7.2
Debye length, λ_D, cm	0.0004
Mean free paths:	
atom-atom, cm	0.017
ion-atom, cm	0.0036
electron-atom, cm	0.067
electron-electron, cm	0.35
electron-ion, cm	0.35
ion-ion, cm	0.007

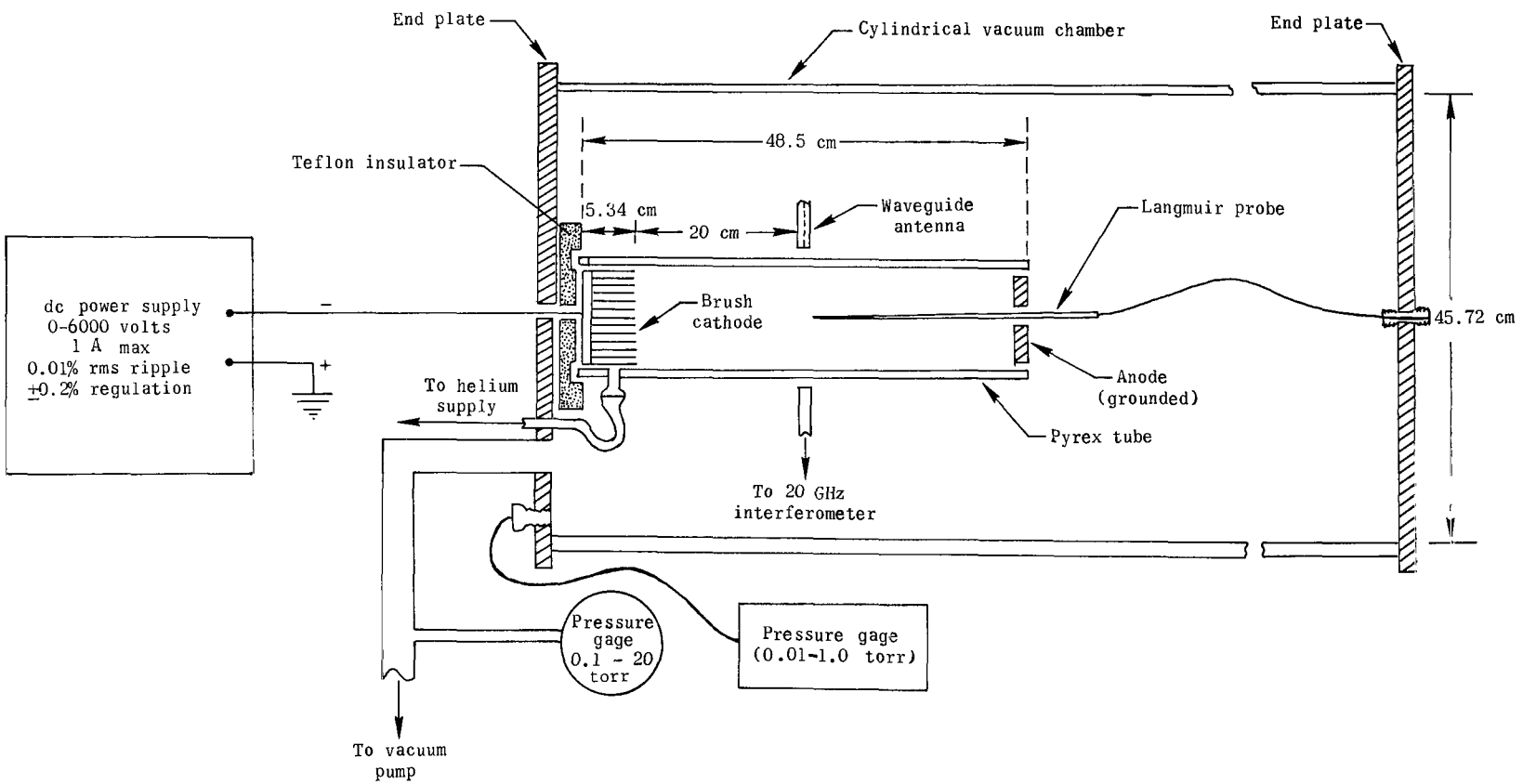

Figure 1.- Schematic diagram of plasma tube (circular cathode installed).

(a) Assembly.

L-67-7248.1

Figure 2.- Plasma tube.

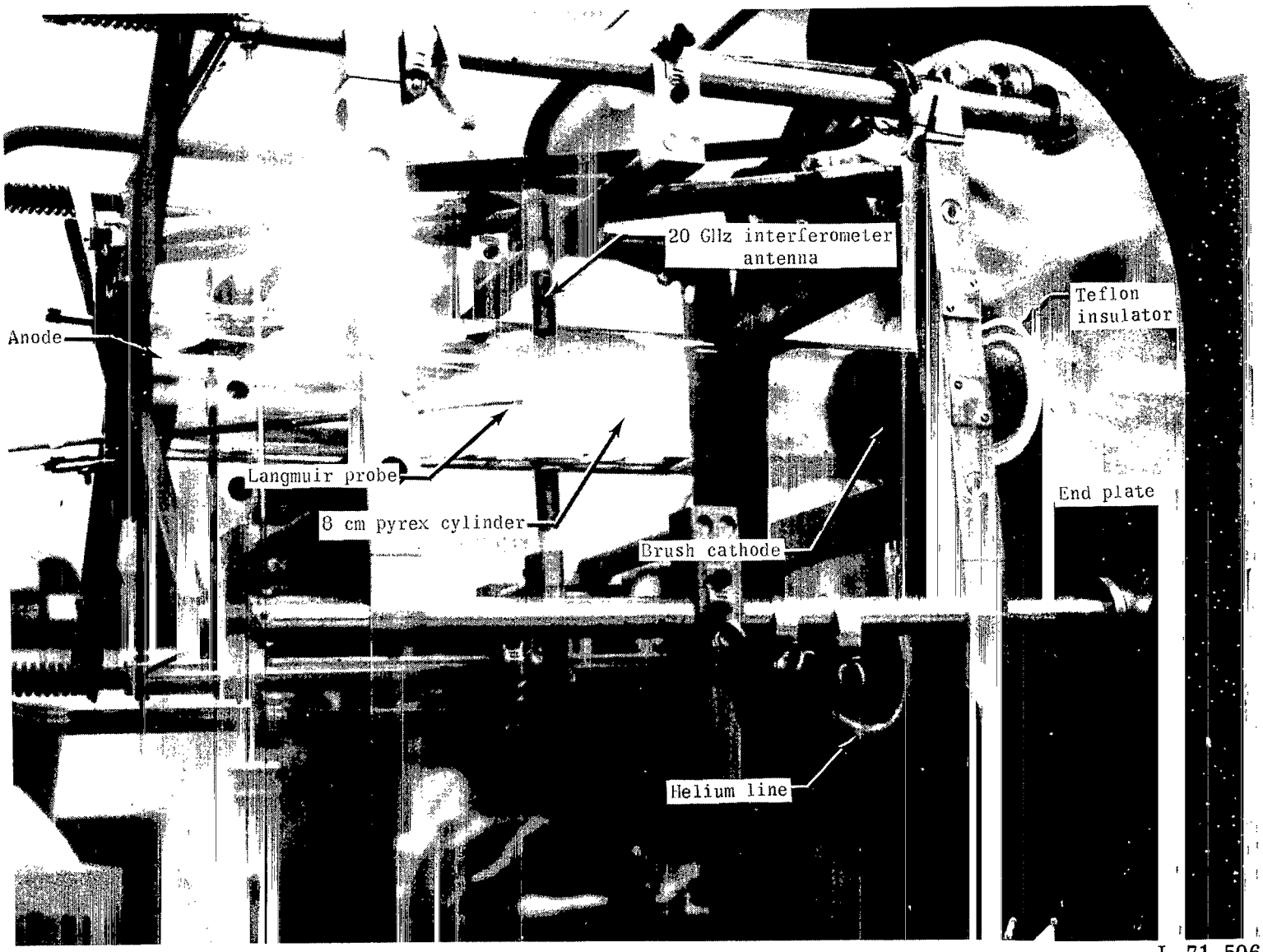

(b) Locations of electrodes and sensors.

Figure 2.- Concluded.

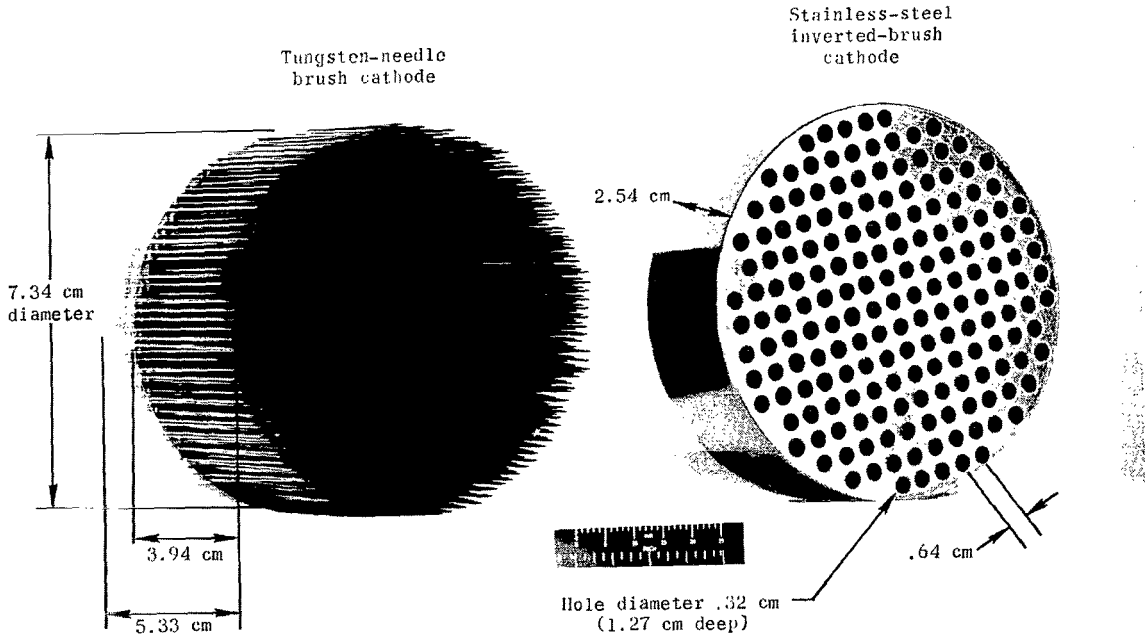

L-67-3480.1

Figure 3.- Circular cathodes.

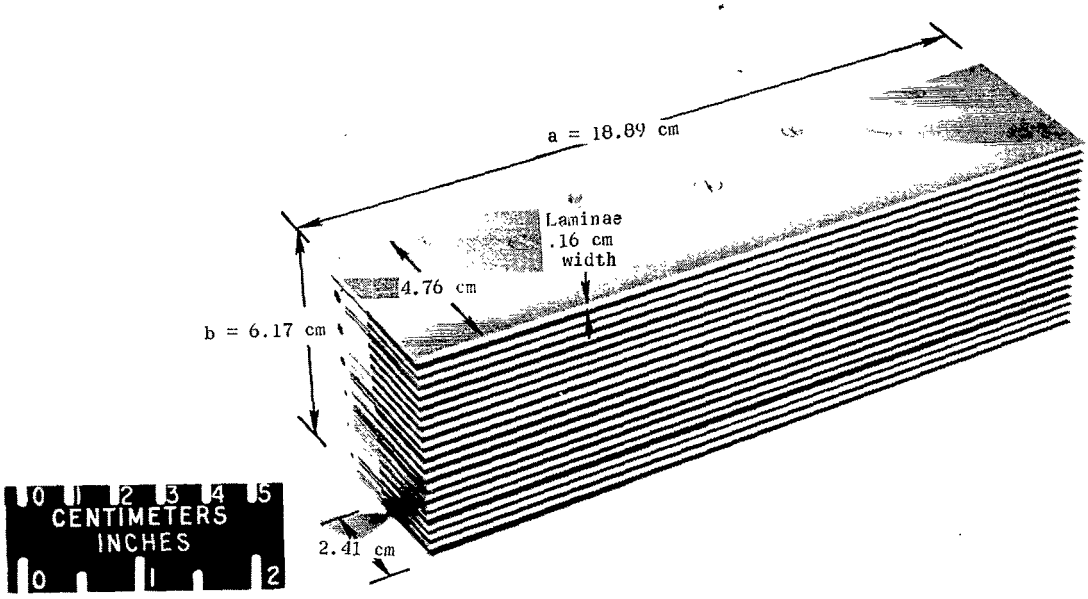

L-67-10027.1

Figure 4.- Rectangular cathode.

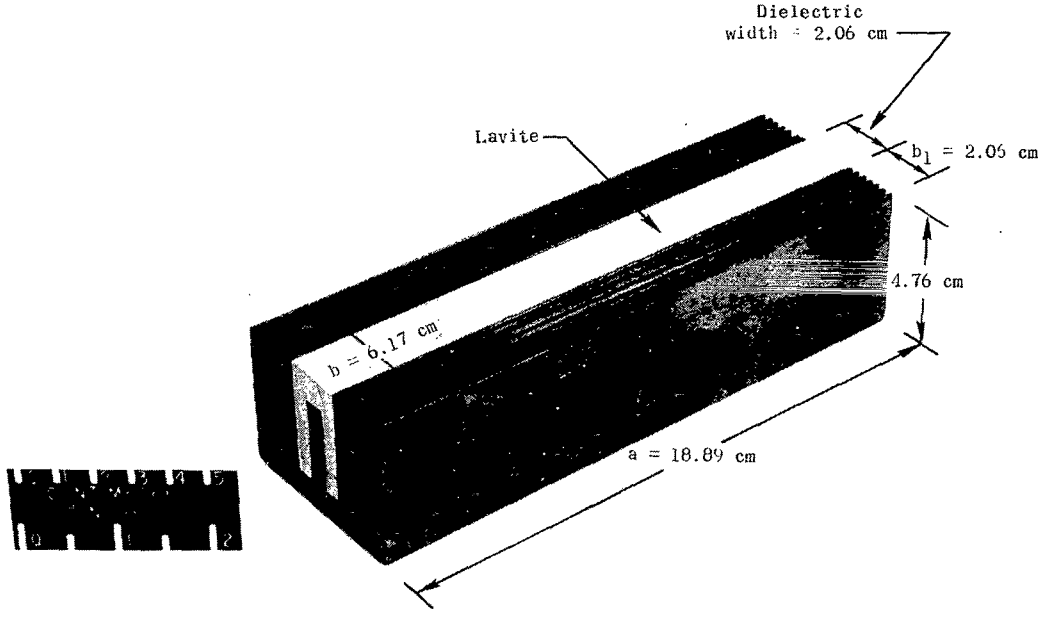

L-67-6430.1

Figure 5.- Rectangular cathode with Lavite insert.

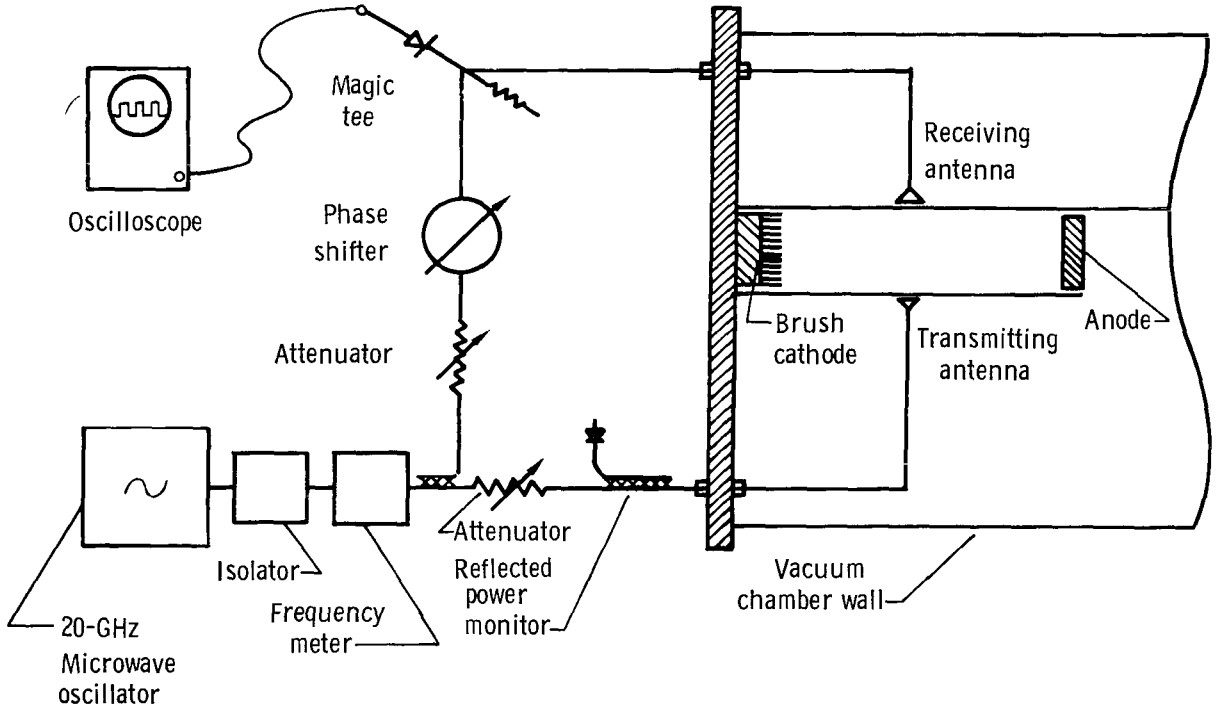

Figure 6.- Block diagram of microwave interferometer.

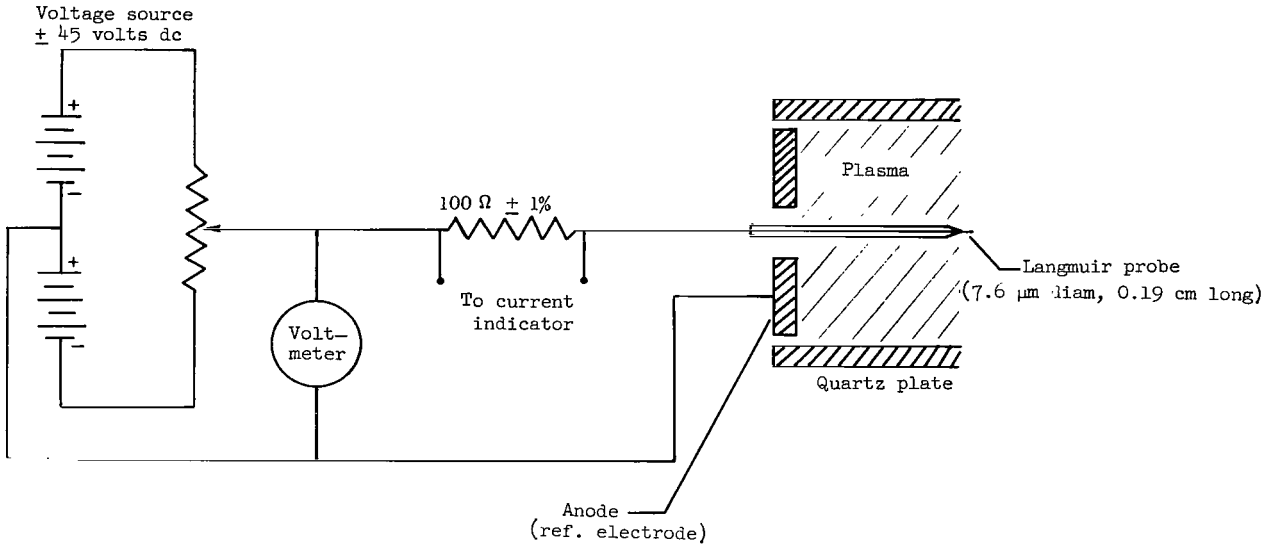

Figure 7.- Langmuir probe circuit.

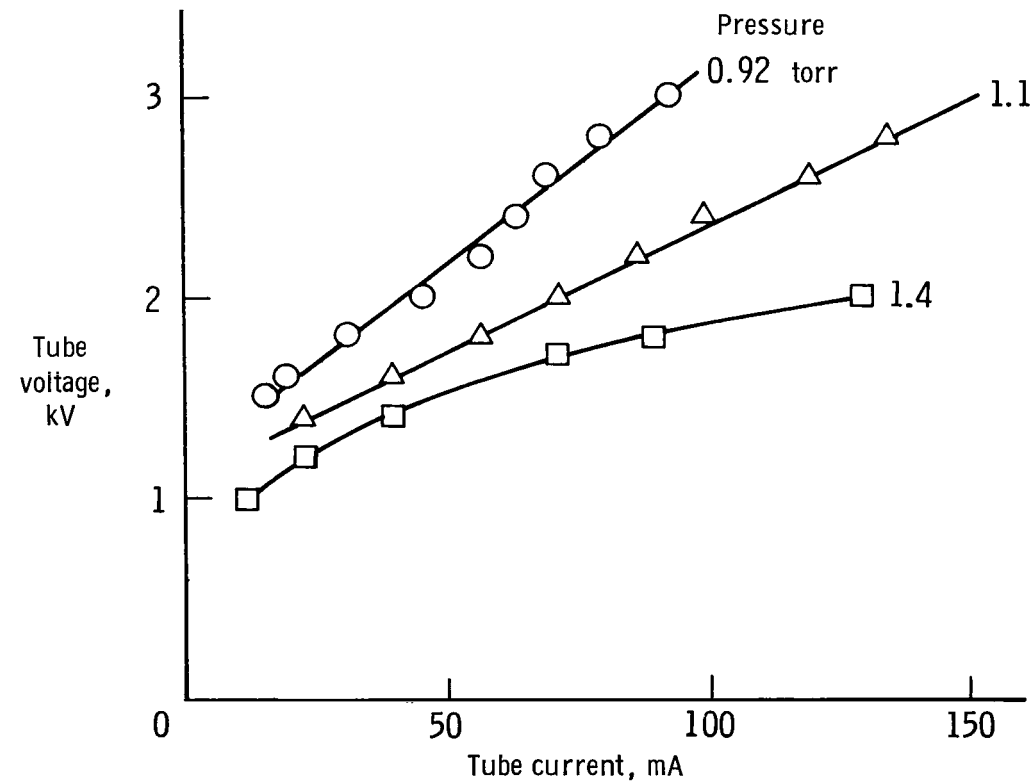

Figure 8.- Voltage-current characteristic for brush-cathode discharge in helium.

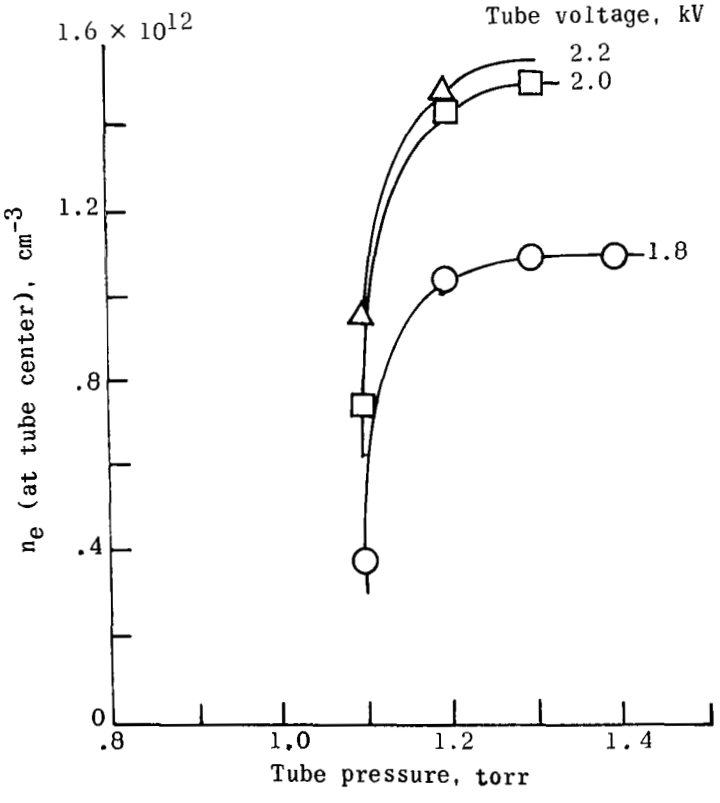

Figure 9.- Electron density from 20-GHz microwave interferometer.

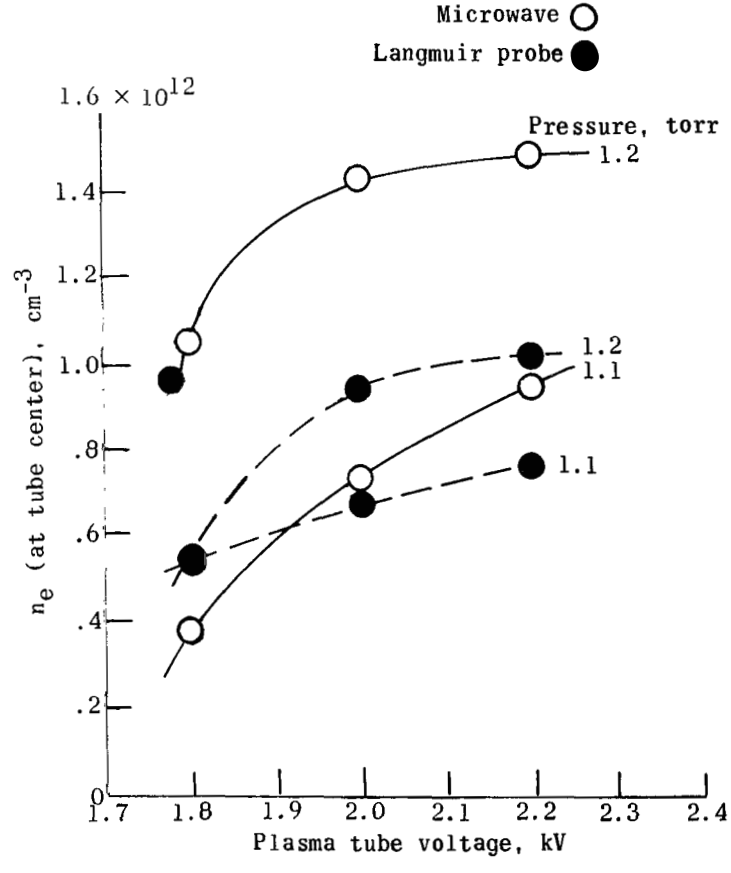

Figure 10.- Plasma electron density measured with Langmuir probe and microwave interferometer.

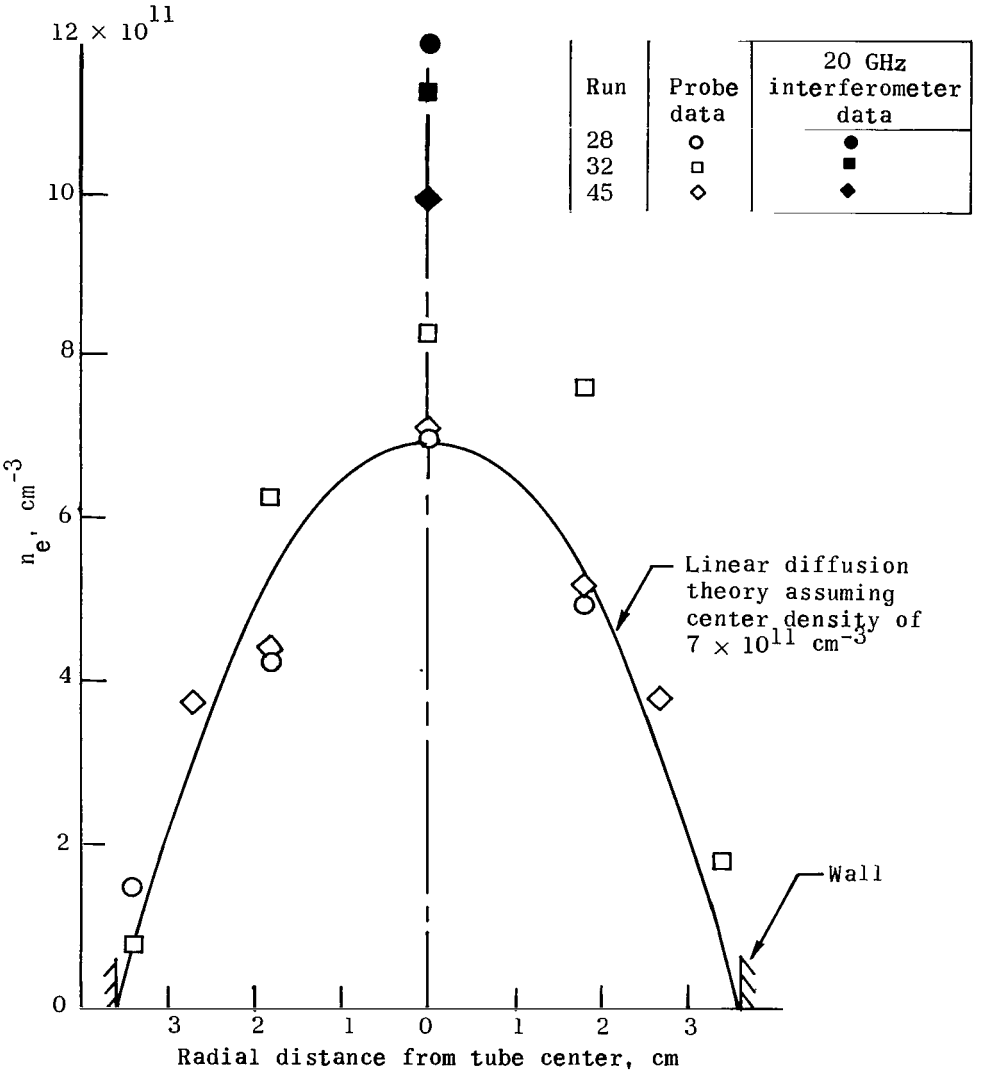

Figure 11.- Radial electron-density profiles from Langmuir probe data.
p = 1.25 torr; V = 1.95 kV.

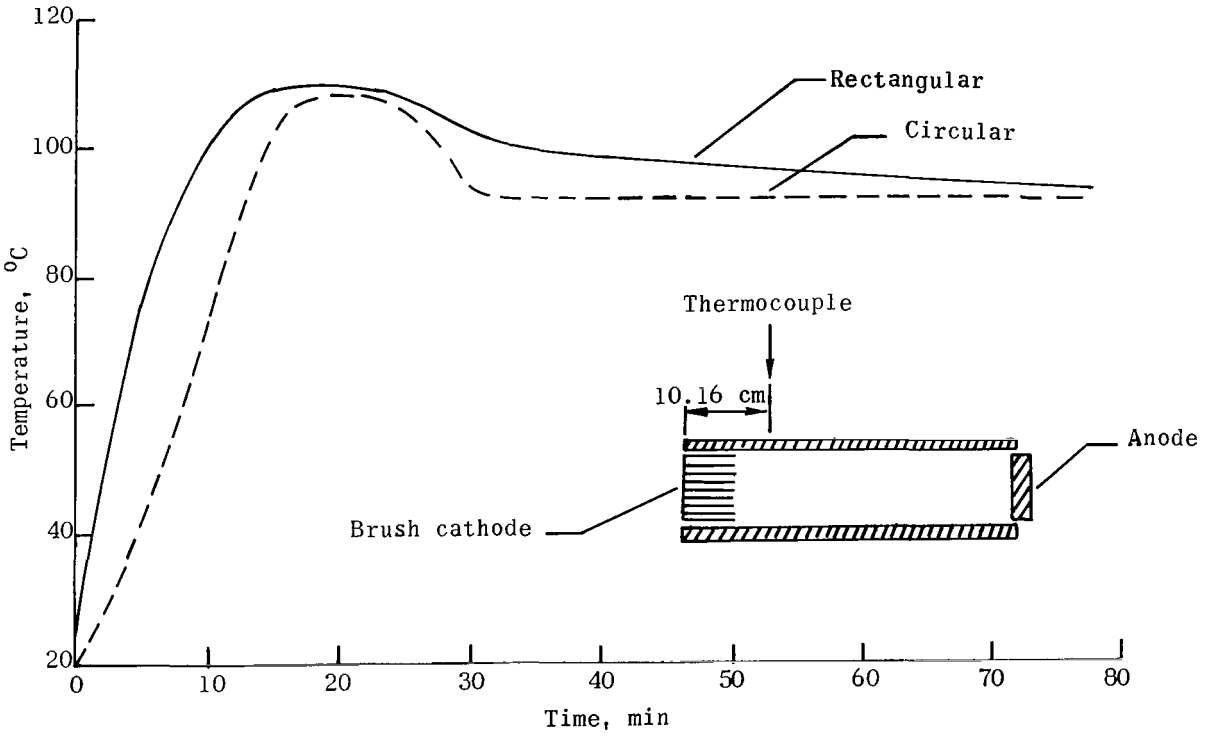

Figure 12.- Temperature time history for plasma tubes.

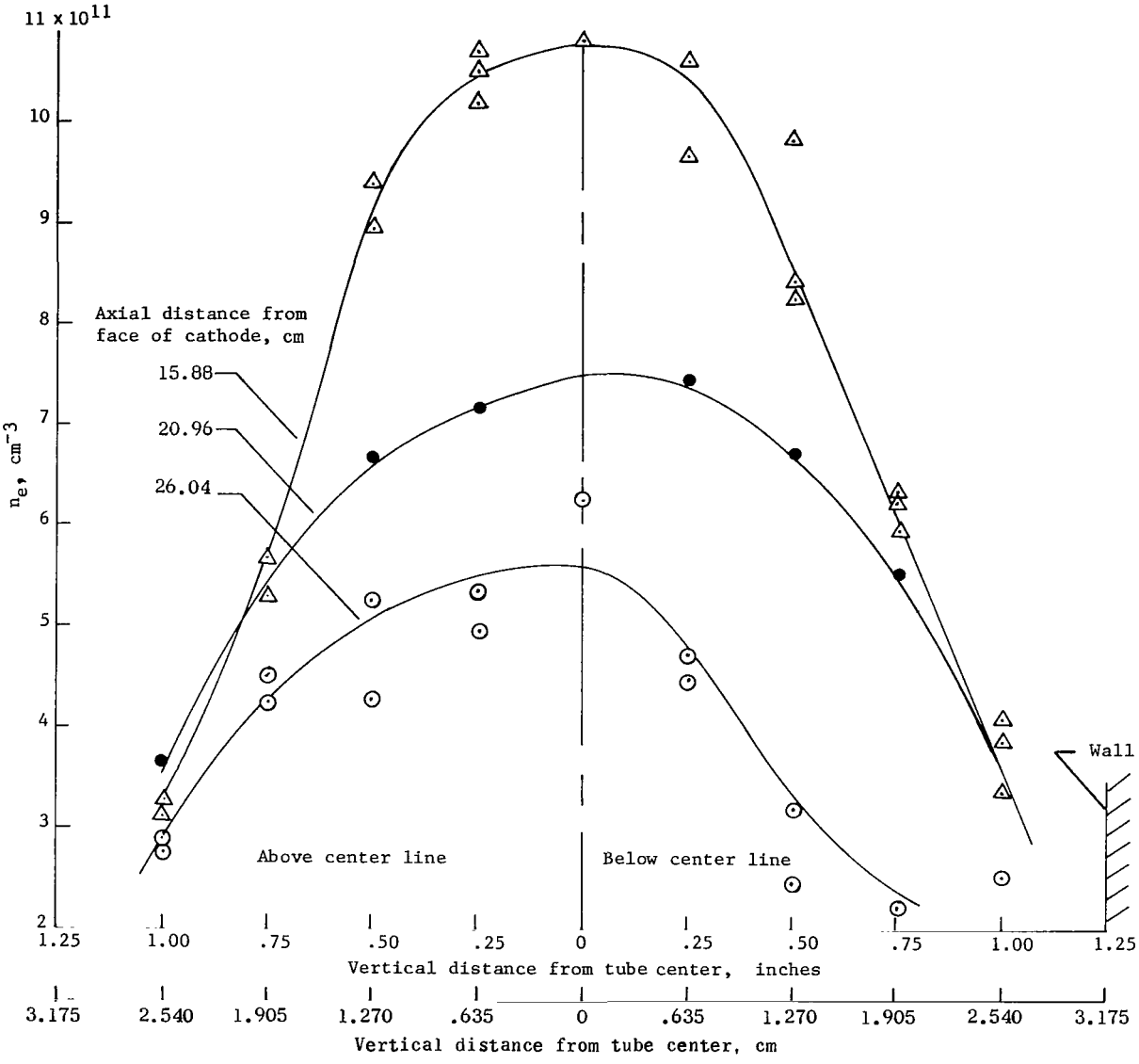

Figure 13.- Plasma electron-density distribution for rectangular cathode configuration at three axial stations. p = 1.25 torr; V = 1.9 kV.

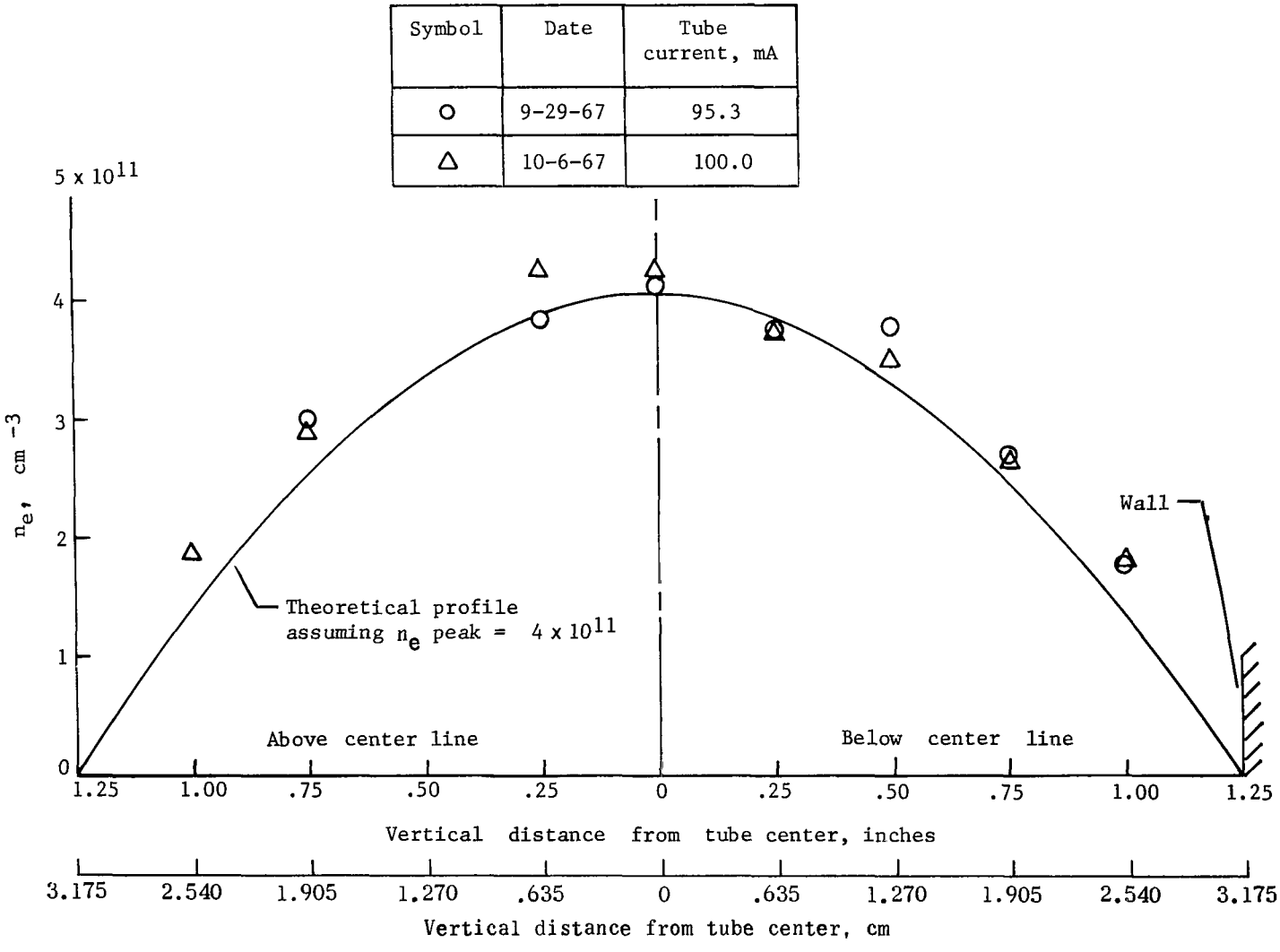

Figure 14.- Electron-density vertical profiles for laminated cathode.
p = 1.25 torr; V = 1.9 kV.

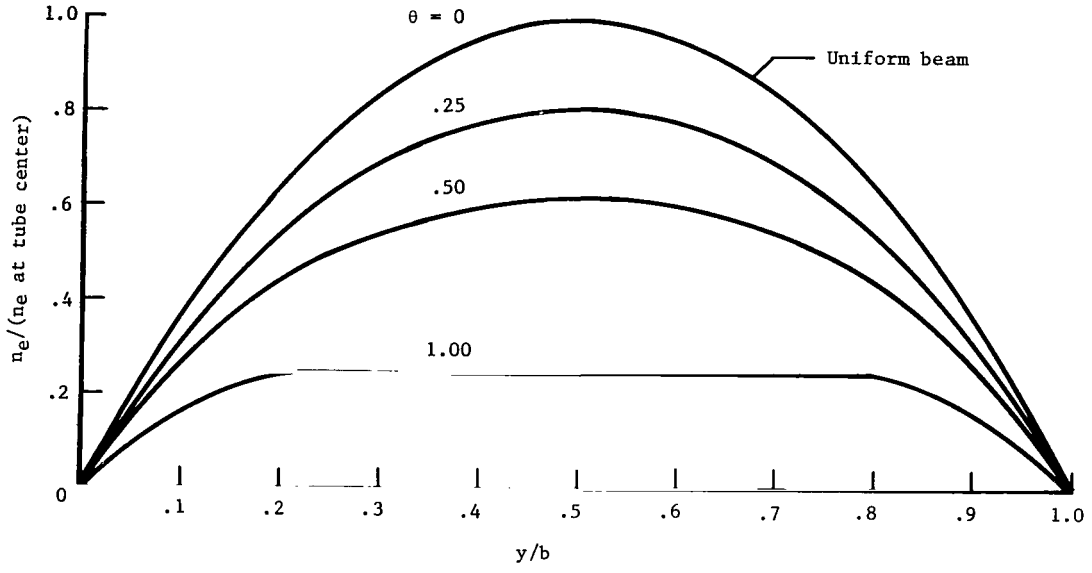

Figure 15.- Theoretical plasma electron-density profiles with a variable source parameter.

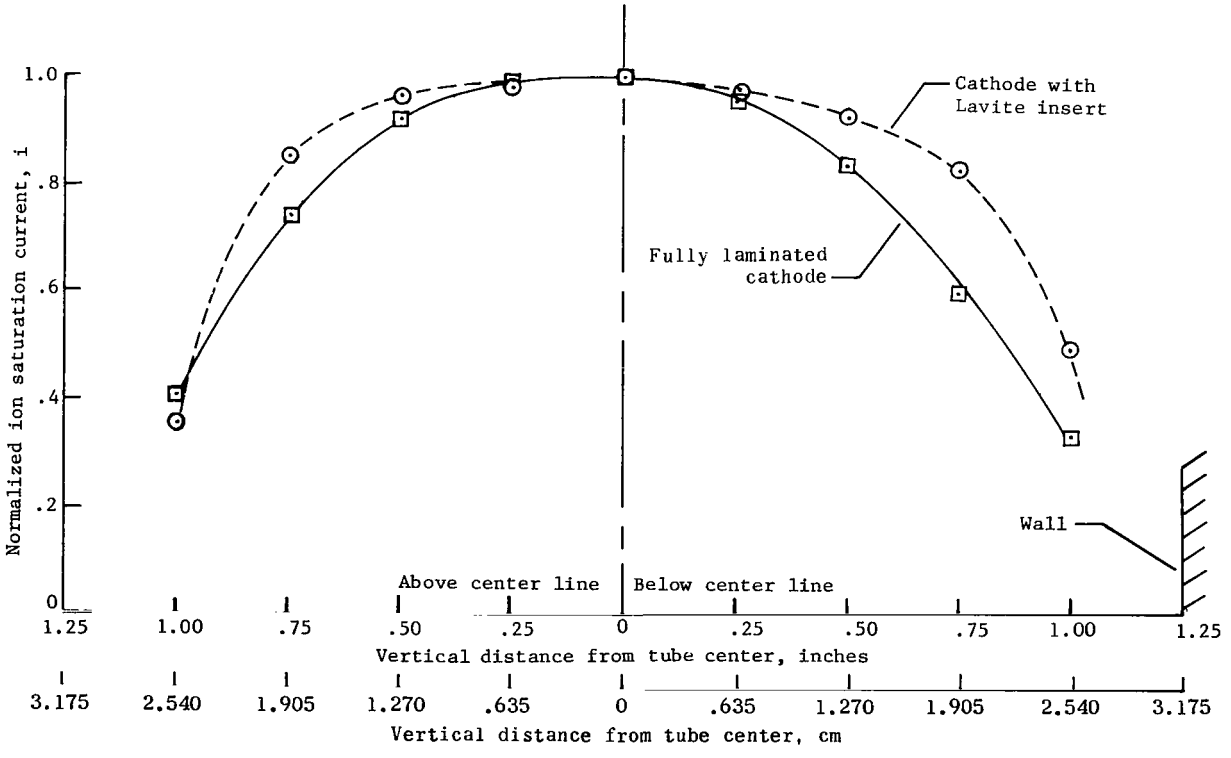

Figure 16.- Plasma profile during tube warmup with and without Lavite insert.

"The aeronautical and space activities of the United States shall be conducted so as to contribute . . . to the expansion of human knowledge of phenomena in the atmosphere and space. The Administration shall provide for the widest practicable and appropriate dissemination of information concerning its activities and the results thereof."

—NATIONAL AERONAUTICS AND SPACE ACT OF 1958

NASA SCIENTIFIC AND TECHNICAL PUBLICATIONS

TECHNICAL REPORTS: Scientific and technical information considered important, complete, and a lasting contribution to existing knowledge.

TECHNICAL NOTES: Information less broad in scope but nevertheless of importance as a contribution to existing knowledge.

TECHNICAL MEMORANDUMS: Information receiving limited distribution because of preliminary data, security classification, or other reasons.

CONTRACTOR REPORTS: Scientific and technical information generated under a NASA contract or grant and considered an important contribution to existing knowledge.

TECHNICAL TRANSLATIONS: Information published in a foreign language considered to merit NASA distribution in English.

SPECIAL PUBLICATIONS: Information derived from or of value to NASA activities. Publications include conference proceedings, monographs, data compilations, handbooks, sourcebooks, and special bibliographies.

TECHNOLOGY UTILIZATION PUBLICATIONS: Information on technology used by NASA that may be of particular interest in commercial and other non-aerospace applications. Publications include Tech Briefs, Technology Utilization Reports and Technology Surveys.

Details on the availability of these publications may be obtained from:

SCIENTIFIC AND TECHNICAL INFORMATION OFFICE

NATIONAL AERONAUTICS AND SPACE ADMINISTRATION

Washington, D.C. 20546